Distribution of Epinemin in Colloidal Gold-labelled, Quick-frozen, Deep-etched Cytoskeletons

DURWARD LAWSON
Department of Zoology, University College London, London WC1E 6BT, United Kingdom

ABSTRACT In this study I describe the ultrastructural distribution of epinemin (Lawson, D., 1983, *J. Cell Biol.*, 97:1891–1905) in antibody-labelled, helium-cooled, quick-frozen, deep-etched cytoskeletons. This technique reveals that epinemin is expressed asymmetrically at discrete sites on the vimentin core polymer and that usually one (occasionally two or three) antiepinemin molecules are found at each of these discrete foci.

Single receptor-bound antiepinemin (IgM) molecules are easily identified in deep-etched cytoskeletons by the use of colloidal gold. Epinemin does not cross-link adjacent intermediate filaments and is not associated with the many 2–3-nm filaments found associated with intermediate filaments in these preparations. The directional changes and interactions undergone by microtubules in taxol-stabilized, antibody-labelled cytoskeletons are also discussed.

The heterogeneous class of intermediate (10-nm diameter) filaments found in eucaryotic cells (see references 18, 22) has been extensively studied by biochemistry (18, 22, 24, 29) and light and electron microscopy (5, 8, 14, 17, 20, 28). The tangled networks formed by these intermediate filaments within cells are made accessible to a variety of antibody probes (see reviews in references 18 and 20) by membrane disrupting agents such as methanol, acetone, and detergents (1, 10, 14, 17).

After detergent extraction, most ultrastructural studies have involved the use of plastic thin sections (1, 14, 17, 20, 30, 31, 34), critical point drying (2, 3, 5, 27–29, 32, 35), or negatively stained isolated filament preparations (6, 37). The artifacts inherent in these techniques are caused by the use of OsO_4 and dehydration steps in preparative protocols. The limitations are, first, the one-dimensional views imposed by thin section electron microscopy and, second, the loss of true structural relationships in isolated filament preparations. The advent of helium-cooled quick freezing (9) and its application to studies of the cytoskeleton (8, 10–12) has meant that these problems can, to a very large extent, be bypassed. Large areas of the cytoskeleton are exposed to view in detergent-extracted Pt-replicated preparations in which it is possible to obtain both scanning type overviews and very high resolution studies of individual filaments and molecules (7, 8, 10–12). By this method, the distribution of intermediate filament core polymers, and their relationship to other cytoskeletal networks, have been studied in various cell systems (8, 10, 12). However, apart from the proteins associated with neurofilaments (10), the many molecules recently found associated with non-neuronal (primarily vimentin) intermediate filament polymers (5, 17–19, 34, 36, 38) have not. The exception, and so far as is known, the only comparable study involves a combination of critical point drying and low angle platinum shadowing to investigate the intermediate filament associated protein synemin in avian erythrocytes (5).

I have previously described a new vimentin associated protein—epinemin—and showed that this molecule was distributed intermittently, in a series of foci, along vimentin filaments in various cells (17). Because of the technical limitations imposed by plastic thin sections, several important points regarding the true distribution and associations of epinemin were impossible to verify. These points are the following: (*a*) whether epinemin is inserted/associated with the vimentin core polymer in a radial, helical, or sided pattern; (*b*) how many molecules of antiepinemin are there at each foci; (*c*) whether antiepinemin has a cross-linking role or is this simply caused by the coincident apposition of foci on adjacent filaments; and (*d*) whether antiepinemin is associated with 2–3-nm filaments (17, 27, 35, 38), or with the attachment site of these filaments on intermediate filaments. These points have been clarified by taking advantage of the unique preservation and three-dimensional views available in helium-cooled, deep-etched cytoskeletons.

In this report I show, for the first time by the method of quick-freezing, the spatial distribution of a vimentin-associated protein, epinemin, on individual filaments within intact cytoskeletons. The presence of this protein on the sides, rather

© The Rockefeller University Press · 0021-9525/84/10/1451/10 $1.00

than completely around intermediate filaments, at foci labelled by one to three antiepinemin IgM molecules is demonstrated by the use of colloidal gold, an electron-dense marker that offers considerable advantages over ferritin in studies involving deep-etched cytoskeletons. In addition, these experiments reveal the extent, and the interweaving, of 2–3-nm filaments, the interaction of intermediate filaments with microtubules, and the changes in direction undergone by microtubules as they associate with various cytoskeletal elements. The difference in size between IgG and IgM molecules is used to give "positive identification" of intermediate filaments labelled with two different antibodies.

MATERIALS AND METHODS

Monoclonal Antibody

Antiepinemin supernatant was produced as previously described (17), harvested, spun at 12,000 *g* for 4 min at room temperature in a Beckman microfuge (Beckman Instruments, Palo Alto, CA), and used immediately for labelling 3T3 cells (see below). Since the class of antiepinemin is IgM (17) there were probably 5–10 μg/ml of monoclonal antibody present (16).

Polyclonal Antibody

Rabbit antivimentin antisera was a kind gift from Richard Hynes (Massachusetts Institute of Technology) and has been previously characterized (14). This antisera was fractionated on DEAE, and the IgG fraction (Rab antivimIgG), which eluted with 40 mM phosphate buffer, pH 7.5, used for these experiments.

Immunofluorescence

This was performed as described (17), except that the Triton X-100 protocol was as detailed in the section *Preparation of Cytoskeletons and Immunocytochemistry* below. The same batch of antiepinemin supernatant was used for the quick-freezing experiments detailed below.

Colloidal Gold Conjugate

Colloidal gold (20 nm) coupled to affinity-purified goat anti-mouse IgG (G anti-mIgG-Au) was purchased from Janssen Pharmaceutica (Beerse, Belgium), and, as recommended by them, spun at 250 *g* for 10 min at 4°C immediately before use to remove possible aggregates. Polyethylene glycol 4000 (PEG 4000)[1] (British Drug House, Dagenham, Essex, England) at a concentration of 0.1% (13) was added to the gold stock solution and to all subsequent diluting media.

Ferritin Conjugate

Goat anti-rabbit IgG (G anti-rabIgG) was coupled to ferritin (FT) by a one-step glutaraldehyde method (G anti-rabIgG-FT) as previously described (23).

Cell Culture

3T3 cells were adjusted to a concentration of 40×10^6 cells/ml in Dulbecco's modified Eagle's medium (DME) plus 10% heat inactivated fetal calf serum, plated overnight in 1-ml aliquots on to 6-mm diameter no. 3 glass coverslips in 24 well Linbro plates and used for all experiments the following day.

Preparation of Cytoskeletons and Immunocytochemistry

ANTIEPINEMIN: G ANTI-MIGG-AU: 3T3 cells were rinsed twice in 0.1 M PIPES plus 1.5 mM $MgCl_2$, 1 mM EGTA pH 6.9 (PIPES), incubated in PIPES for 1–3 min at 37°C, and then extracted for 3–10 min at 37°C in 0.5% Triton X-100 in PIPES plus 2 μg/ml taxol (26) (supplied by Natural Products Branch, Division of Cancer Treatment, National Institutes of Health), which was included until cytoskeletons were in glutaraldehyde. Cytoskeletons were then rinsed four times in PIPES, fixed in 1% stabilized formaldehyde (British Drug House) in PIPES for 10 min at 37°C, rinsed four times in PIPES plus 20 mM lysine, and once in PIPES/lysine plus 0.1% bovine serum albumin (BSA) (Pathocyte Five Miles Research Products Division, Elkhart, IN). Coverslips were then incubated at 20°C with 18 μl of antiepinemin supernatant (or supernatant from a nonsecreting hybridoma—both plus taxol and lysine as above), rinsed five times in PIPES/lysine, fixed in 0.1% glutaraldehyde in PIPES for 30 s and then placed in 1 ml of PIPES for 5–10 min at 20°C. Samples were rinsed three times in 20 mM Tris, pH 8.2, plus 20 mM lysine and once in Tris/lysine plus 0.1% BSA, incubated in 18 μl of G anti-mIg-Au diluted 1:5 in Tris/lysine/0.1% BSA/0.1% PEG 4000 for 30 min at 20°C, rinsed three times in Tris/lysine/BSA/PEG, once in Tris and either fixed in 1% glutaraldehyde in PIPES for 1 h at 20°C and stored in PIPES at 4°C or subsequently processed as below.

ANTIEPINEMIN: G ANTI-MIGG-AU: RAB ANTI-VIMIGG: After labelling as above, samples were rinsed with Tris/lysine/BSA/PEG and then incubated in 18 μl of 0.5 mg/ml Rab anti-vimIgG in Tris/lysine for 30 min at 20°C, rinsed in Tris, fixed in glutaraldehyde, and stored as above.

RAB ANTIVIMIGG: G ANTI-RAB IGG-FT: Coverslips of 3T3 cells were extracted, labelled with 1 mg/ml Rab anti-vimIgG followed by G anti-rabIgG-FT, rinsed, fixed, and stored in glutaraldehyde all exactly as above.

Quick Freezing: Freeze Drying and Replication: Freeze Substitution

Cells were stored in PIPES at 4°C for 1 to 24 h, rinsed in double distilled deionized water, then 15% methanol, and quick frozen at temperatures ranging from 6 to 10°K (see below). The freezing head and sample were immediately plunged into liquid nitrogen, the frozen sample removed and (*a*) stored in liquid nitrogen or (*b*) fitted on to a modified Balzers freezing head and placed in a Balzers BAF 400D (Balzers, Hudson, NH) using the rapid side-load system. Samples were etched for 1 h at temperatures ranging from −95°C to −87°C in a vacuum of better than 5×10^{-7} torr. In some experiments they were lightly scraped, and then etched at −95° to −87°C for 20–30 min. All samples were replicated with platinum and carbon and processed as described (8). Replicas were viewed in a Jeol 100 CXII operating at 100 kV with a ±60° tilt side entry goniometer. Micrographs are printed from reversal negatives (8) unless otherwise stated. Freeze substitution was by standard methods.

Quick-Freezing Machine: The "guillotine" framework of the machine used for these experiments is based on the photograph of a freezing machine on the cover of a "rapid freezing parts catalogue" very kindly sent to me by J. E. Heuser (Washington University) in 1978. The dimensions and the plan for the machine built at University College London were drawn by E. J. Lawson. The machine was built by Keith Smith (University College London) and the following points were incorporated in its design. To avoid precooling the specimen, I reduced the depth between the top of the upper cold block and the cold chamber to 5 mm. The freezing head has a spring/plunger arrangement incorporating a simple rubber shock absorber arrangement to reduce the oscillations inherent in any undampened spring. This effectively stops the sample moving fractionally on the copper cold block when the freezing head hits the electromagnet. The time between the sample hitting the copper cold block and the freezing head hitting the electromagnet is easily altered by varying the plunger length. The copper cold block is as light as possible to facilitate rapid cooling (~15 s from 20°C to −267°C [6°K]) and is designed so as to incorporate a calibrated potted carbon thermistor (Cryogenic Calibrations, Pitchcott, Bucks, United Kingdom) 3 mm below its surface. Thus, the temperature recorded (accurate to better than 0.5°K) is as nearly as possible the temperature at the top of the copper cold block where the sample freezes. A potted carbon thermistor (rather than a thermocouple) is used for greater accuracy at lower temperatures. The freezing rate signal (recorded for every experiment) is measured as a reduction in capacitance and is recorded on equipment based on the information published by Heuser et al. (9).

RESULTS

A prerequisite for these studies was to show that frozen cells were free from ice crystal damage. Fig. 1 shows that the top 10 μm of tissue are frozen in 1 ms or less, a rate that is known to yield well frozen specimens (9). Furthermore, it can be seen that the structural preservation of fibroblasts, frozen at this speed, and then freeze substituted, is excellent with no visible ice crystal damage (Fig. 2). The cytoplasm of such cells is notably dense, packed full of organelles and contains a thick closely woven feltwork of filaments (Fig. 2).

To reveal the in-depth views of the cytoskeleton obtainable by deep etching, I extracted fibroblasts in Triton X-100 and

[1] *Abbreviations used in this paper:* BSA, bovine serum albumin; FT, ferritin; PEG, polyethylene glycol.

then froze them similarly. To obtain the maximum resolution from deep etched replicas and avoid the presence of large sheets of membrane that obscured the underlying cytoskeletons, it was necessary to use higher concentrations of Triton X-100 than were used for thin section electron microscopy (17). Longer times in Triton X-100 also helped remove much of the cytoplasmic debris that otherwise stuck nonspecifically to the cytoskeletons. However, some of this debris remained, even after 10 min in 0.5% Triton X-100, and caused problems in unequivocally identifying small clusters of antibody (see Discussion).

Vimentin Labelling

Fibroblasts contain many intermediate filaments recognized in Pt replicas by their smooth appearance and overall diameter (for example, see reference 8 and Fig. 5). However, to compare the appearance of deep-etched intermediate filaments decorated along their entire length and around their circumference by antibody with those decorated intermittently by antiepinemin, I labelled Triton X-100–extracted fibroblasts with Rab anti-vimIgG followed by G anti-rabIgG-FT. This greatly facilitated tracing intermediate filaments, now thickened and completely coated by FT, as they wove beside microtubules and actin stress fiber bundles (Fig. 3). These cells (in which the microtubules had been stabilized with taxol) showed the close relationship that exists between intermediate filaments and microtubules. In Fig. 3, it is apparent that intermediate filaments are in close contact with the microtubule framework. The microtubules (and possibly the intermediate filaments) invariably bend (often quite acutely) not only at these points of apparent contact with intermediate filaments (Fig. 3) but when they are in close juxtaposition to other microtubules (Fig. 3). Control cells incubated with 1 mg/ml RabIgG then G anti-rabIgG-FT were unlabelled (not shown).

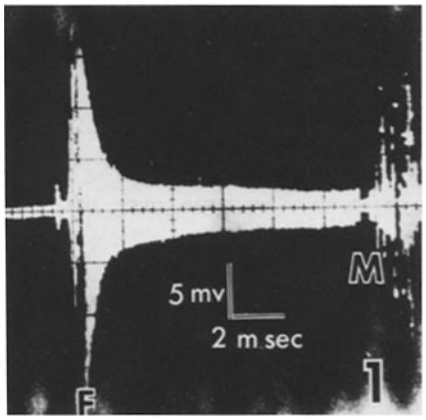

FIGURE 1 Freezing rate measurement, seen as a reduction in capacitance when water turns to ice, from a typical experiment. Sample hits the cold block and freezes (*F*) and then the freezing head hits the magnet (*M*). The trace shows that the top 10 μm of tissue freezes in ~1 ms. For details of this methodology see reference 9.

Epinemin Labelling

For all these experiments, fresh antiepinemin supernatant was used and, by immunofluorescence, gave the wavy staining pattern typical of the vimentin filament network (Fig. 4), see reference 17. A similar cytoskeletal view, but in fibroblasts labelled with antiepinemin followed by G anti-mIgG-Au is seen in Fig. 5, *a* and *b*. Here a tangle of intermediate filaments is studded by Au particles that delineate the epinemin foci clearly. These foci are randomly distributed along intermediate filaments as previously described (17) and while clusters of up to four to six Au particles are seen, many Au particles are distributed as singlets (Fig. 5, *a* and *b*). Deep etching now makes it possible to see that all antiepinemin foci are found at the sides, rather than completely around the circumference, of the vimentin core polymer (Fig. 5, *a* and *b*). (Similar results were found even when 3 mg/ml of antiepinemin were used [not shown].) This is very clear at high magnification where the "inverted bucket" shape (4, 25) of one IgM (the class of antiepinemin) labelled with Au can be seen sitting on the side of a single vimentin filament (Fig. 6). No individual Fab arms were ever seen in these experiments (Fig. 6). That the orientation of the filament relative to the direction of view and the size of the IgM/G anti-mIgG-Au complex were not obscuring other antiepinemin molecules attached underneath the filament at the same foci was shown by tilting the replica through 120° (not shown).

Interactions of Epinemin

These results also show that the larger clusters and rows (seen in Fig. 5, *a* and *b*) of Au particles are due to the proximity

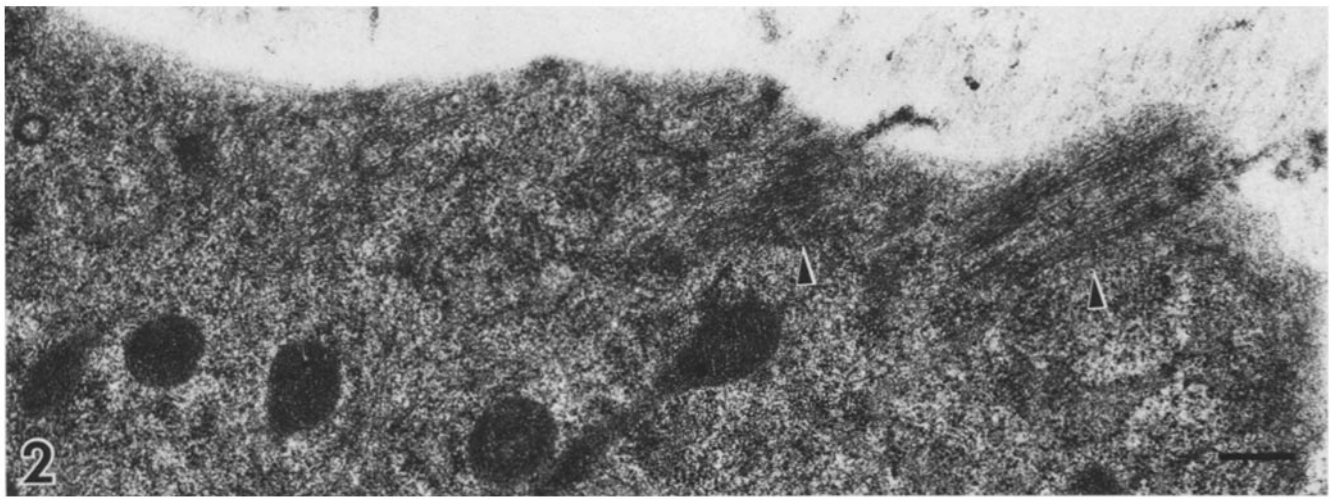

FIGURE 2 Oblique section of a quick-frozen, freeze-substituted fibroblast with no visible ice crystal damage. A dense network of filaments can be seen extending to the cell periphery (arrowheads). Bar, 300 nm. × 32,000.

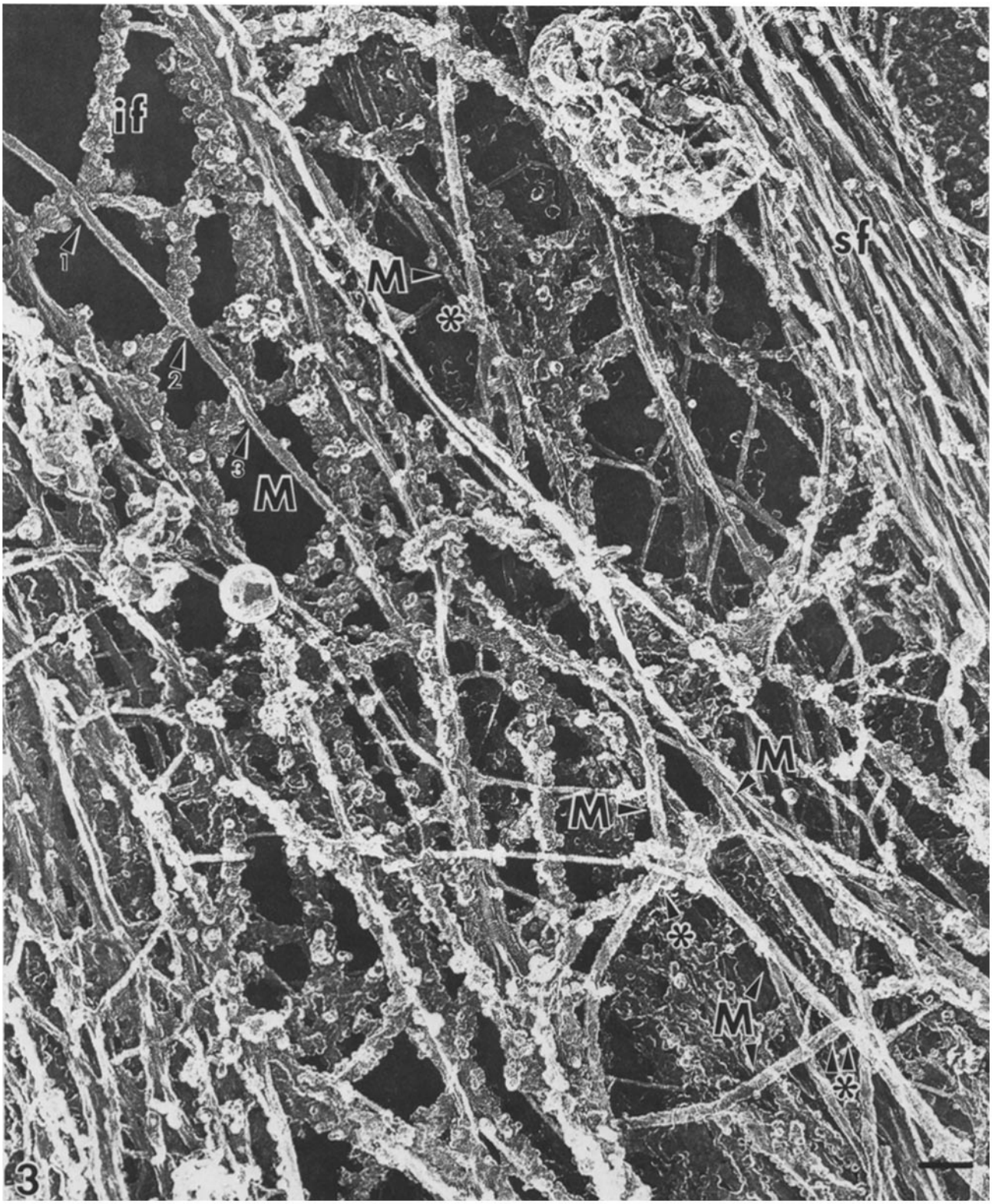

FIGURE 3 Replica of a fibroblast extracted with Triton X-100 then labelled with Rab anti-vimIgG followed by anti-rab FT, quick frozen and then deep etched. Intermediate filaments (*if*), thickened and studded all around their circumference by knobs of FT, form a complex network weaving around and beside microtubules (*M*) and actin, a stress fiber bundle (*sf*) of which can be seen at the outside of the cell. Microtubules and intermediate filaments are in close physical contact at many points (arrowheads *1*, *2*, and *3* and arrowhead plus asterisk). Note that microtubules bend at these points of interaction. Where microtubules are closely juxtaposed they also change direction (asterisk), occasionally quite acutely (double arrowhead plus asterisk). Bar, 100 nm. × 83,000.

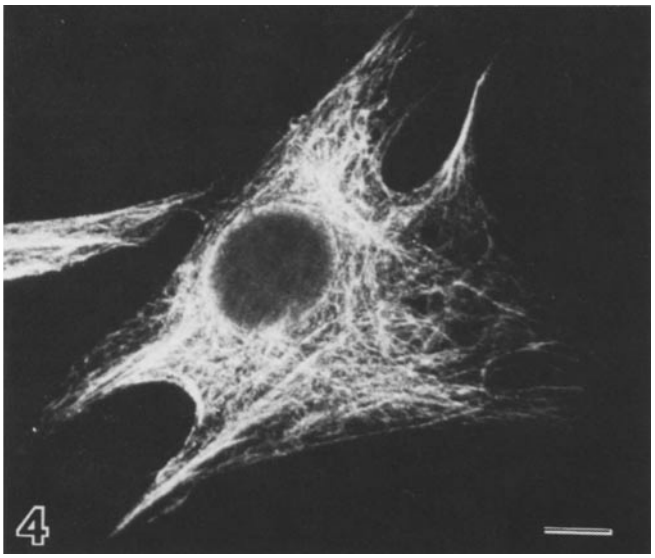

FIGURE 4 Triton X-100 extracted fibroblast labelled with antiepinemin supernatant showing a wavy filamentous network. Bar, 10 μm. × 730.

of antiepinemin foci on adjacent filaments (Fig. 7). Little evidence of any lateral registry between antiepinemin foci was ever found in these studies (Figs. 5, *a* and *b*, 7, and 9), therefore any apparent bridging of antiepinemin is clearly due to the random coincident apposition of antiepinemin foci on adjacent (often parallel) filaments (Fig. 7). That for steric reasons (see discussion) one or at most two Au particles can bind to one antiepinemin, coupled with the measurements of individual antiepinemin molecules themselves (see discussion) suggests that when intermediate filaments are close together this apparent bridging is possible with only two antiepinemin IgMs, one on each filament (Fig. 7). When the filaments are further apart the same apparent bridging phenomenon is given by 2–3 IgMs on each filament (Fig. 7). This gives the larger cluster size of about six Au particles seen in these experiments (Figs. 5, *a* and *b*, 7, and 9).

Many 2–3-nm filaments were found in these preparations forming a delicate web draped over and around mainly intermediate filaments (Figs. 7 and 8). This web of 2–3-nm filaments is composed of single strands of various lengths (Figs. 7 and 8) and, interestingly, also adopts an X-like configuration between intermediate filaments (Figs. 7 and 8).

Deep etching shows that no antiepinemin is found either labelling 2–3-nm filaments themselves or where they interact with intermediate filaments (Figs. 7 and 8).

Positive Identification

To unequivocally identify vimentin filaments, I labelled them in sequence with antiepinemin, G anti-mIgG-Au, and then Rab anti-vim-IgG. This "positive identification" (rather than the "negative identification" of a different filament type: in this case actin with S1—see Discussion) coated the vimentin filaments with a rough layer of IgG molecules (seen also in the elegant work of Heuser and Kirschner [8]) out of which appear the heads of the antiepinemin IgM molecules labelled with G anti-MIg-Au (Fig. 9). Antiepinemin was found only on antivimentin coated filaments (clearly indicating the specificity of the reagents) and here too the foci are found only at the sides of vimentin filaments (Fig. 9). In addition, G anti-mIg-Au was found neither on the actin geodomes present in cells labelled as above (not shown) nor on cells labelled with supernatant from a nonsecreting hybridoma and then G anti-mIgG-Au (not shown).

Finally, while most samples were etched for long periods it seems unlikely that any of the filaments described in this study were the result of salt deposition (21) because (*a*) in all experiments previously characterized antibodies were used to label intermediate filaments and it seems unlikely these would recognize filaments formed from salt, (*b*) all cytoskeletons were rinsed in distilled water and methanol before freezing: a protocol which eliminates salts and the artifactual appearance of filaments (21).

DISCUSSION

These studies were undertaken in an attempt to clarify, by using antibody-labelled, helium-cooled, deep-etched cytoskeleton, points raised in a previous paper (17) concerning the "in depth" distribution and relationships of epinemin.

Intermediate Filaments and Microtubule Interactions

The first series of experiments were initially aimed simply at optimizing the conditions for visualizing antibody-labelled intermediate filaments in Triton X-100–extracted, quick-frozen, deep-etched cytoskeletons. To accomplish this, I labelled intermediate filaments with an antivimentin (which has previously been shown to cover them completely [8]) followed by a FT coupled second antibody. In this instance FT was added (*a*) to further roughen the outline of intermediate filaments, (*b*) to allow easy low magnification tracing of their pathways and interactions as they coursed through the cytoskeleton, and (*c*) to show the difference in appearance between intermediate filaments labelled completely around their circumference by antibody and electron-dense marker with those where the antibody and electron-dense marker were distributed asymmetrically (see below). The most interesting (and unexpected) bonus from these experiments was how clearly they showed the relationships existing between microtubules and intermediate filaments. For this, taxol was essential to preserve microtubules and maintain cytoskeletal integrity. This is not surprising when the symbiotic relationship known to exist between microtubules and intermediate filaments (14, 15, 17–20) is looked at by deep etching.

These studies show that intermediate filaments drape over microtubules and are probably in contact with them at many points. That microtubules form a molecular scaffold for intermediate filaments (not for actin microfilaments) and not vice versa is suggested by the use of microtubule depolymerizing drugs that collapse microtubules and intermediate filaments (14, 17–19) and by microinjection studies using monoclonal antibodies against intermediate filaments, and associated proteins, which collapse intermediate filaments but not microtubules (15, 20). While the results contained in this report show apparent contact (almost always seen as a directional change in microtubules) between this molecular scaffold of microtubules and intermediate filaments, they do not tell us if the collapse of intermediate filaments because of microtubule depolymerization is (*a*) nonspecific and due simply to the loss of a mechanical framework, (*b*) specific and mediated by a linkage molecule between the two networks, or (*c*) a combination of these factors. In line with these

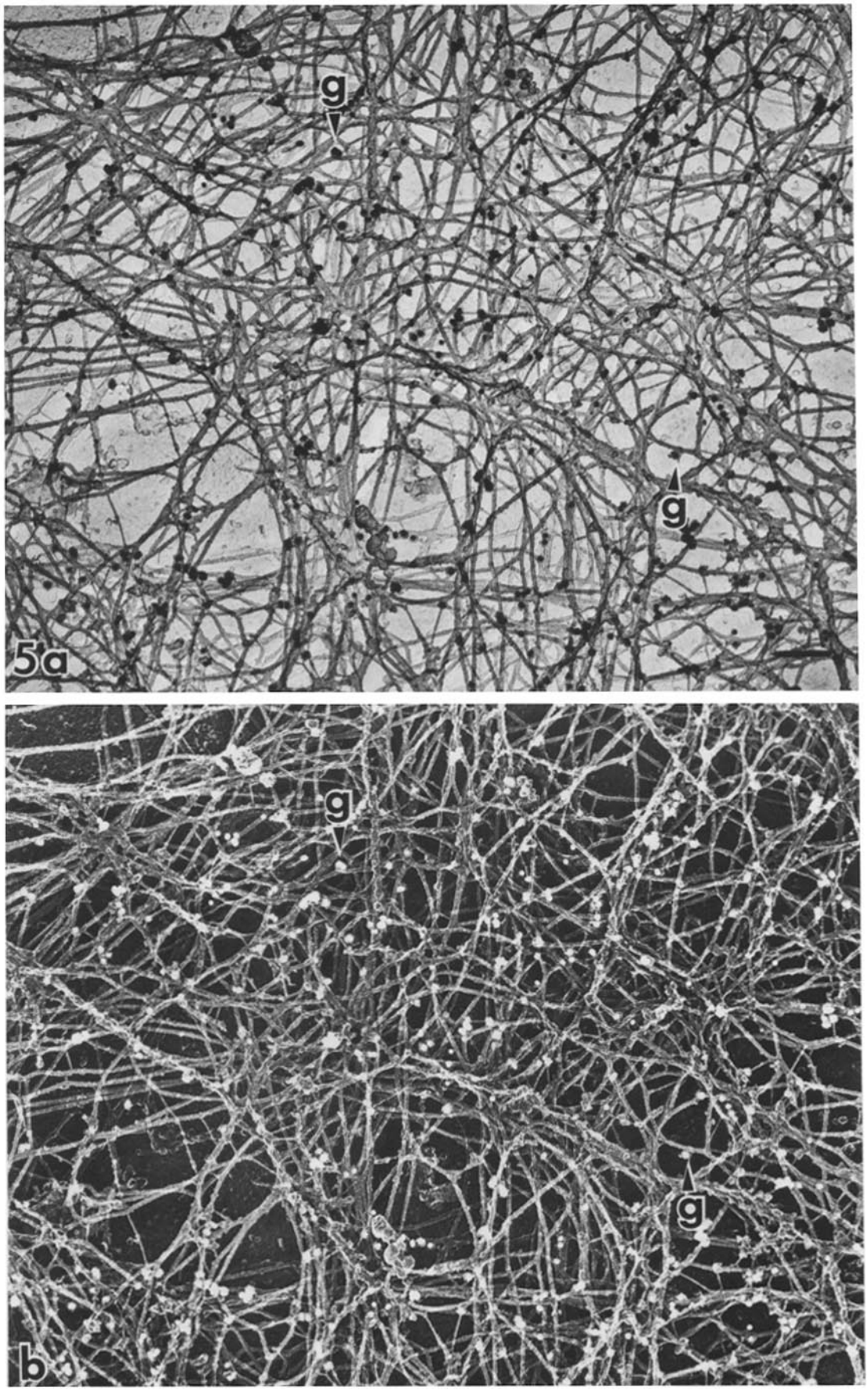
g
g
5a
g
g
b

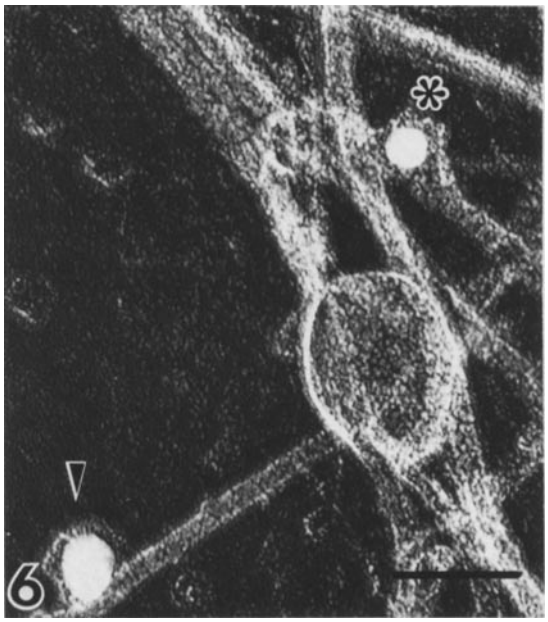

FIGURE 6 High power image of antiepinemin/Au labelling intermediate filaments. Very occasionally the inverted bucket shape of an IgM molecule could be seen (asterisk), but more often than not Au particles labelled structures of a more amorphous shape (arrowhead). The asymmetric distribution of antiepinemin is clearly seen. Bar, 50 nm. × 320,000.

observations, actin/microtubule interactions were not notable in these experiments and those that were present did not appear to alter the direction taken by microtubules as they coursed through the cytoskeleton. In contrast, microtubules do appear to change direction when they are in contact with either intermediate filaments or another microtubule. It seems unlikely that this was caused by antibody binding, since the cytoskeletons were aldehyde-fixed before each antibody layer. The acute directional changes in microtubules seen in these experiments confirms that the similar observations of Schliwa and van Blerkom (28) were not induced by critical point drying. That bends are seen in microtubules suggests that the precise arrangement of tubulin subunits in the microtubule wall varies at these points.

Antiepinemin

In preliminary experiments to determine the spatial distribution of epinemin, I used no electron-dense marker since it has been shown that unlabelled antibody can be seen in quick frozen deep-etched replicas (8). However, two factors militated against following this approach. First, even high concentrations of Triton X-100 left amounts of cytoplasmic debris adhering to the cytoskeleton. Second, and directly related to this was the distribution of epinemin itself, it proving difficult to unambiguously differentiate between small foci of antiepinemin and small aggregates of debris. This made the use of an electron-dense marker a necessity. FT's low electron density and rough appearance in deep-etched replicas (reference 12 and these results) meant that it was relatively easy to confuse with particles of debris and, as a result, was less suitable for identifying small numbers of molecules distributed in discrete foci. On the other hand, 20-nm Au particles proved almost ideal, highlighting the antiepinemin foci and allowing scanning type overviews in which the distribution of antibody could still be easily seen while the high resolution capability of Pt replicas meant that individual antibody molecules themselves could then be looked at in detail.

These experiments showed that epinemin foci are distributed asymmetrically at the sides of vimentin filaments. No radial or helical type distribution (1, 31, 37) was ever seen. The possibility that other antiepinemin/Au complexes were present at the same foci, but out of the visual plane, was excluded by tilting replicas through 120°. Although it is possible that molecules of epinemin remained unlabelled, even at the high antibody concentration used for some experiments, the fact that a ring of antiepinemin was never seen around intermediate filaments strongly suggests that the true distribution of epinemin is at discrete foci which are asymmetrically expressed on the vimentin core polymer. In these and previous studies (17) the degree of labelling by antiepinemin varied considerably on different intermediate filaments. No explanation has so far been found for this. That a uniform distribution of epinemin is seen by light, but not electron, microscopy is very likely due to the limited resolution (0.2–0.3 μm, see reference 36) of light microscopy. Similar results have been found for another intermediate filament associated protein (5).

At many of these foci only one IgM molecule was found: an observation verified by measurements of individual IgM molecules after quick freezing (see also reference 7), by tilt electron microscopy, and by the number of Au particles that can bind to one antiepinemin (see below). However, while the "inverted bucket" shape of IgM (4, 25) could occasionally be seen, no individual Fab_1 arms were ever resolved in these studies. This may have been caused by either glutaraldehyde fixation or freezing damage; but while the former cannot be excluded, the latter seems unlikely because (*a*) the speed and quality of freezing has been demonstrated, and (*b*) it has been shown that Fab_1 arms are visible as individual entities on isolated IgM molecules frozen on mica flakes (7). That this configuration of IgM was not more frequently seen may also be because some of the Fab_1 arms of IgM are not attached to epinemin receptors. They would thus be free to move and would very likely then collapse and distort during the processes of aldehyde fixation and freezing, giving rise to the amorphous shape of the IgM molecule more usually seen in these studies. Alternatively, it seems equally likely that as the IgM molecule grasps the filament/receptor complex, like a "bird's claw" on a branch (adopting the table configuration with the Fc disk on top [1, 4, 25]), the Fab_1 arms move so closely together that they cannot be singly resolved in a Pt replica. These results also suggest that this bird's claw arrangement of IgM does not so much clasp round the filament as

FIGURE 5 (*a*) Replica of a fibroblast extracted with Triton X-100, labelled with the same antiepinemin supernatant as Fig. 4, then G anti-mIgG-Au quick frozen and deep etched. A tangle of intermediate filaments is seen, labelled in a random pattern with Au particles, many of which are present as singlets. Of the rest, the largest cluster size comprises approximately six Au's. That the Au/antiepinemin complexes are found at the side, not around, intermediate filaments can be seen even at this low magnification (*g* arrowhead). This micrograph is printed as it looked down the microscope to show how clearly Au particles can be seen. Bar, 200 nm. × 47,600. (*b*) Reversal image of *a* to show filaments more clearly.

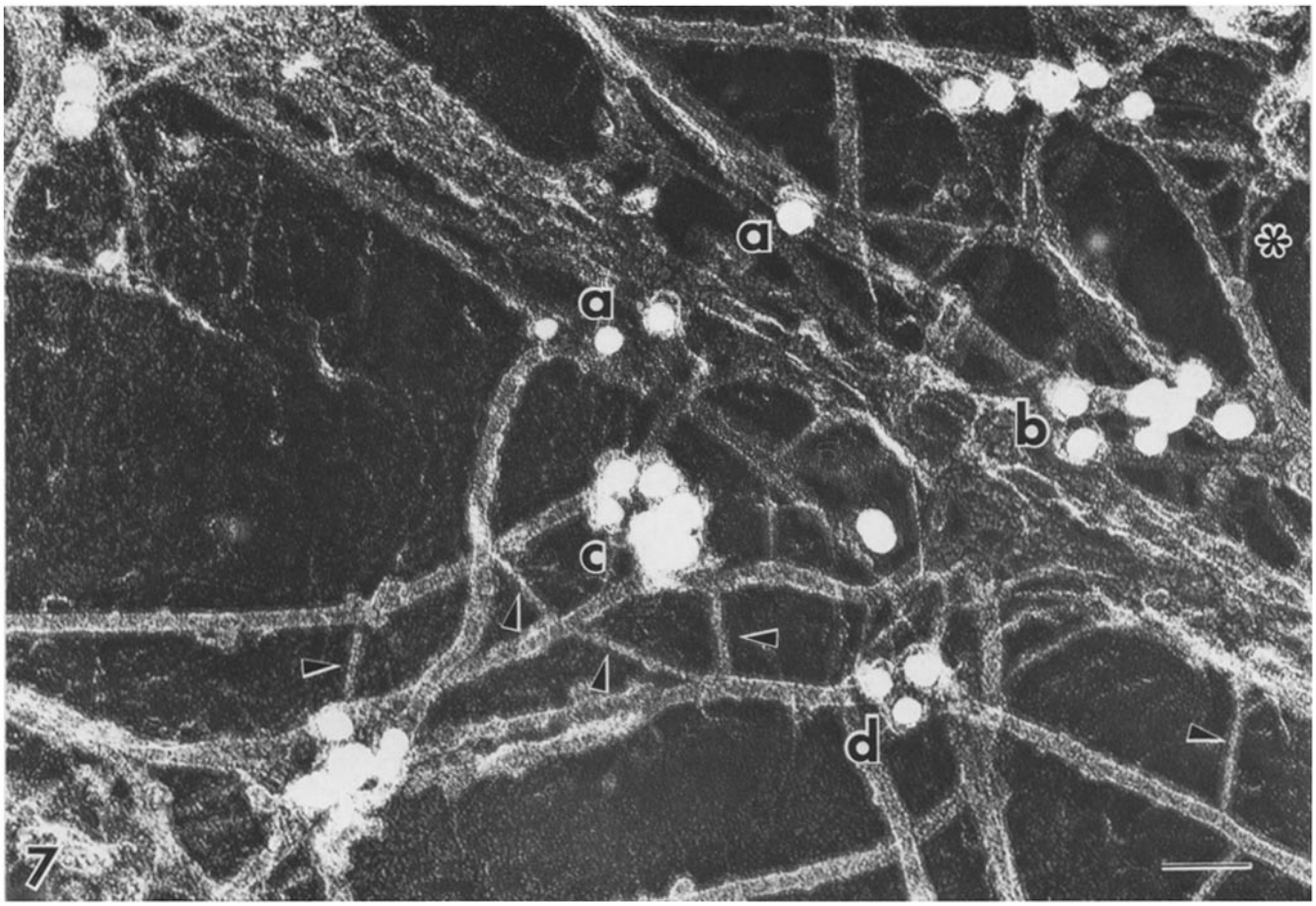

FIGURE 7 Antiepinemin labelled deep etched fibroblast. Most foci of antiepinemin do not exhibit lateral registry (seen at *a*). Apparent bridging occurs only when these foci become randomly apposed on adjacent filaments. In this situation only one antiepinemin IgM on each filament is necessary when the filaments are close together (seen at *b*) and two to three IgMs on each filament when they are further apart (seen at *c*). A cluster of up to two to three antiepinemin molecules is seen *en face* at *d*. Intermediate filaments are draped over and probably around by 2–3-nm filaments (arrowheads) which also adopt an X-like configuration (asterisk). Bar, 50 nm. × 240,000.

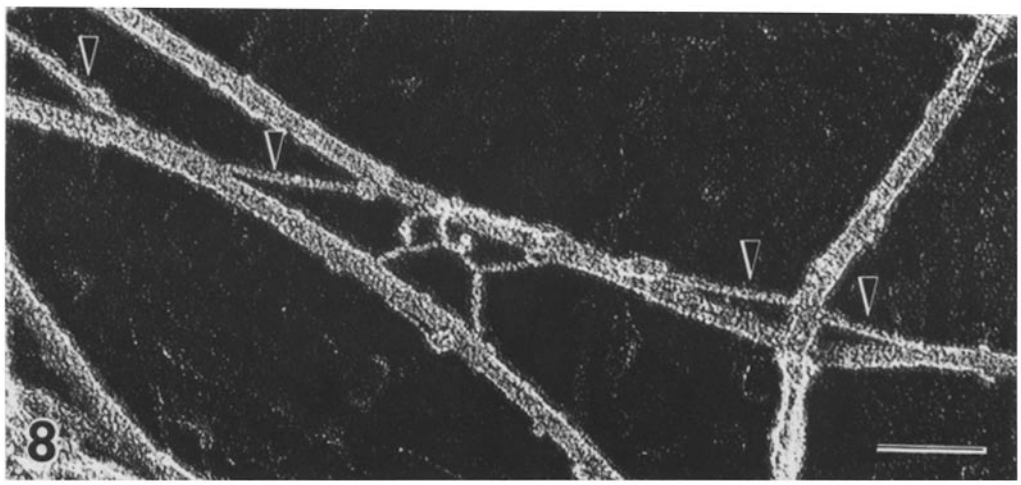

FIGURE 8 High power micrograph of 2–3-nm filaments (arrowheads) draped over and along intermediate filaments. The X shape occasionally adopted by these small filaments is clearly seen. Bar, 50 nm. × 280,000.

perch on it: a configuration that may be in line with the expression of epinemin over a limited area at the side of a filament.

The size of the Au particles (20 nm on average), plus their surrounding shell of IgG molecules (diameter of one IgG molecule ~12 nm [4, 7, 25]) giving an overall diameter for the Au/IgG complex of ~40 nm, suggests that with this Au size class, for steric reasons, on average only one or two Au/

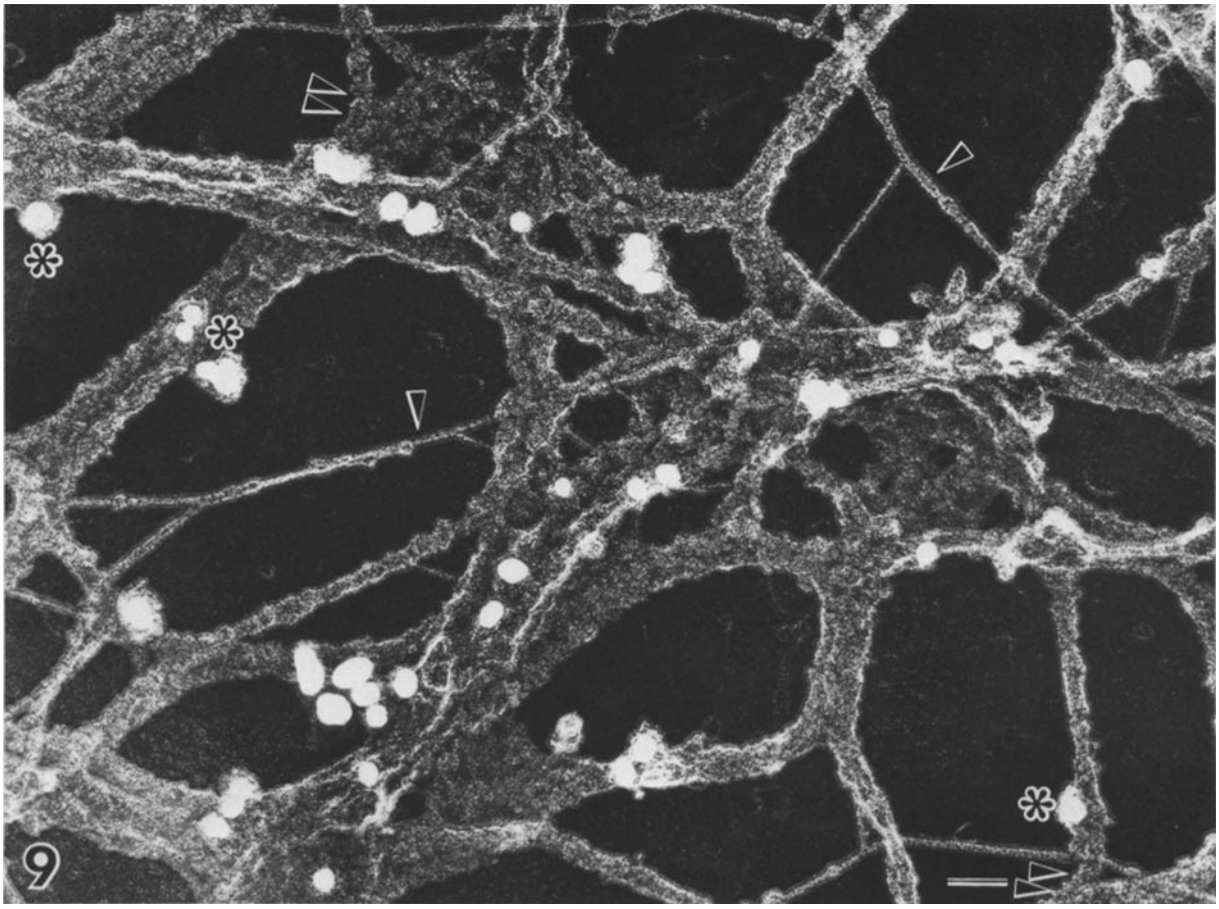

FIGURE 9 Positive identification of intermediate filaments in a deep etched fibroblast labelled in sequence with antiepinemin, G anti-mIgG-Au then Rab anti-vimIgG. Intermediate filaments are completely coated and roughened by the antivimentin IgG (double arrowheads). Out of this layer of IgG appear the heads of the antiepinemin IgM/Au molecules (asterisks), the asymmetric expression of which is still easily seen. Filaments uncoated by antivimentin (arrowheads) are unlabelled by antiepinemin. Bar, 50 nm. × 168,000.

IgG can bind to one IgM, a view that is substantiated by the tilting experiments mentioned above. With this relationship, the lack of any lateral registry between epinemin foci and the size of IgM in mind, it is now possible, by deep etching, to look at any putative cross-bridging phenomena mediated by epinemin. It seems clear, from these data, that this is a result of (*a*) the size of a given Au/IgM complex, (*b*) the distance between adjacent intermediate filaments, and (*c*) whether or not epinemin foci are by chance in coincident apposition as intermediate filaments pass near each other. Epinemin does not therefore appear to have any real cross bridging role that has been suggested for another intermediate filament-associated protein (5).

2–3-nm Filaments

In my hands, this intriguing class of filaments (17, 27, 28, 35) was relatively difficult to visualize in plastic thin sections and previously their relationship to epinemin remained ambiguous (17). However, by deep etching, it can be seen that while antiepinemin foci and 2–3-nm filaments are found very close to each other, antiepinemin is not associated with them, or their points of interaction with intermediate filaments, in any apparent way. The importance of taxol in preserving microtubules, and as a result the integrity of the intermediate filament network with its associated filigree-like network of 2–3-nm filaments, cannot be overemphasized.

In deep-etched replicas, it was very easy to trace the pathways of 2–3-nm filaments as they wove through the intermediate filament network. 2–3-nm filaments not only drape over intermediate filaments, they also appear to weave around them and, interestingly, to adopt an X-like configuration between adjacent intermediate filaments. No other filament type seen in these studies ever displayed this type of delicate X lattice shape. These small filaments are nonactin-like because of (*a*) their size, (*b*) their lack of the striped appearance characteristic of actin in Pt replicas (8, 12; and these results), and (*c*) the fact that they do not bind S1 (28). In other cell types, the primary association of small filaments with actin (11, 33) suggests the existence of a ubiquitous family of small cross-linking filaments. While the role of this fourth cytoskeletal network remains unknown their principal association, in these experiments, with intermediate filaments suggests that they may be involved in the equally unknown role of this latter class of filaments. Possibly 2–3-nm filaments convert intermediate filaments into a functionally cross-linked syncytium.

Filament Identification

It has been convincingly demonstrated that actin filaments in deep-etched replicas exhibit a characteristic striped pattern

possessed by neither intermediate filaments nor microtubules (8, 12; and these results). The latter are also easily identified on the basis of their large size. However, to identify unequivocally actin the S1 head of myosin has been used as a decorating molecule that gives a characteristic rope-like appearance to actin filaments (8, 11, 12). The disadvantage of this form of labelling (unless the interest is in actin filaments themselves) is the severe distortion that S1 causes in the cytoskeleton, and while aldehyde fixation has been shown to minimize this, it does not stop the breakage/loss of fine connecting filaments ([12] and personal observation). It seems probable that S1 causes this damage by unkinking, straightening, and breaking the numerous bends and Y-shaped connections that actin makes within the cytoskeleton.

Therefore, to allow easy distinction between actin and intermediate filaments, I used the difference in size between IgG and IgM, and the unique specificity of antibodies, to do double-label, deep-etch experiments. This meant that when cytoskeletons were labelled in sequence with antiepinemin (IgM), G anti-mIgG-Au, and then Rab anti-vim-IgG, islands of large IgM molecules (with associated Au particles) identifying the antiepinemin foci were seen only in a surrounding sea of smaller antivimentin IgG molecules covering all the intermediate filaments. The advantage of this technique (which might also be applied to other filaments and their associated proteins) is that the cytoskeletons could be stabilized in up to 1% glutaraldehyde before labelling with the polyclonal antivimentin. This effectively minimizes damage to small cross-linking filaments and helps to maintain overall cytoplasmic integrity. While under investigation, a functional role for epinemin, in common with nearly all other intermediate filament associated proteins and intermediate filaments themselves, still remains conjectural.

Many thanks to John Heuser (Washington University, St. Louis) for sending a catalogue of parts which enabled me to instigate building the freezing machine used for these studies and Norton B. Gilula (Baylor College, Houston) for laboratory space while introducing me to the technique of freeze fracture. I also thank E. J. Lawson for drawing the plans for the freezing machine, Keith Smith (Physics Department, University College London, [UCL]) for his expertise in building and modifying all the mechanical parts, Mervyn Hardiman (Medical Research Council, Neural Mechanisms of Behaviour Unit, UCL) for building the electronics and Stuart Bevan (Zoology Department, UCL) and Peter de Villiers (Biophysics Department, UCL) for their advice on the many problems we encountered here. It is always a pleasure to thank Stefanello de Petris (Zoology Department, UCL) and Rhona Mirsky (Anatomy Department, UCL) for their interest in and constructive criticisms of this work, and Peter Harwood for his excellent technical assistance.

This work was supported by a project grant from the Medical Research Council.

Received for publication 2 April 1984, and in revised form 6 July 1984.

REFERENCES

1. Blose, S. H., F. Matsumura, and J. J. C. Lin. 1981. Structure of vimentin 10-nm filaments probed with a monoclonal antibody that recognizes a common antigenic determinant on vimentin and tropomyosin. *Cold Spring Harbor Symp. Quant. Biol.* XLVI:455–463.
2. Boyles, J., and D. F. Bainton. 1979. Changing patterns of plasma membrane associated filaments during the initial phases of polymorphonuclear leukocyte adherence. *J. Cell Biol.* 82:347–368.
3. Ellisman, M. H., and K. R. Porter. 1980. Microtrabecular structure of the axoplasmic matrix: visualisation of cross-linking structures and their distribution. *J. Cell Biol.* 87:464–479.
4. Feinstein, A., and D. Beale. 1977. Models of immunoglobulins and antigen-antibody complexes. *In* Immunochemistry: An Advanced Textbook. Glynn and Steward, editors. John Wiley & Sons, London. 263.
5. Granger, B. L., and E. Lazarides. 1982. Structural associations of synemin and vimentin filaments revealed by immunoelectron microscopy. *Cell.* 30:263–27.
6. Henderson, D., N. Geisler, and K. Weber. 1982. A periodic ultrastructure in intermediate filaments. *J. Mol. Biol.* 155:173–176.
7. Heuser, J. E. 1983. Procedure for freeze-drying molecules adsorbed to mica flakes. *J. Mol. Biol.* 169:155–195.
8. Heuser, J. E., and M. W. Kirschner. 1980. Filament organization revealed in platinum replicas of freeze-dried cytoskeletons. *J. Cell Biol.* 86:212–235.
9. Heuser, J. E., T. S. Reese, M. J. Dennis, Y. Jan, L. Jan, and L. Evans. 1978. Synaptic vesicle exocytosis captured by quick freezing and correlated with quantal transmitter release. *J. Cell Biol.* 81:275–300.
10. Hirokawa, N. 1982. Cross-linker system between neurofilaments, microtubules, and membranous organelles in frog axons revealed by the quick-freeze, deep-etching method. *J. Cell Biol.* 94:129–142.
11. Hirokawa, N., and L. G. Tilney. 1982. Interactions between actin filaments and between actin filaments and membranes in quick-frozen and deeply etched hair cells of the chick ear. *J. Cell Biol.* 95:249–261.
12. Hirokawa, N., L. G. Tilney, K. Fujiwara, and J. E. Heuser. 1982. Organization of actin, myosin and intermediate filaments in the brush border of intestinal epithelial cells. *J. Cell Biol.* 94:425–443.
13. Hopkins, C. R., and I. S. Trowbridge. 1983. Internalization and processing of transferrin and the transferrin receptor in human carcinoma A.431 cells. *J. Cell Biol.* 97:508–521.
14. Hynes, R. O., and A. T. Destree. 1978. 10 nm filaments in normal and transformed cells. *Cell.* 13:151–163.
15. Klymkowsky, M. W. 1981. Intermediate filaments in 3T3 cells collapse after intracellular injection of a monoclonal anti-intermediate filament antibody. *Nature (Lond.).* 291:249–251.
16. Köhler, G. 1981. The Technique of Hybridoma Production: Immunological Methods II. Academic Press, Inc., London. 284–298.
17. Lawson, D. 1983. Epinemin: a new protein associated with vimentin filaments in non-neural cells. *J. Cell Biol.* 97:1891–1905.
18. Lazarides, E. 1982. Intermediate filaments: a chemically heterogeneous developmentally regulated class of proteins. *Annu. Rev. Biochem.* 51:219–250.
19. Lin, J. J. C. 1981. Monoclonal antibodies against myofibrillar components of rat skeletal muscle decorate the intermediate filaments of cultured cells. *Proc. Natl. Acad. Sci. USA.* 78:2335–2339.
20. Lin, J. J. C., and J. R. Feramisco. 1981. Disruption of the *in vivo* distribution of the intermediate filaments in fibroblasts through the microinjection of a specific monoclonal antibody. *Cell.* 24:185–193.
21. Millar, K. R., C. S. Prescott, T. L. Jacobs, and N. L. Lassignal. 1983. Artefacts associated with quick-freezing and freeze drying. *J. Ultrastruct. Res.* 82:123–133.
22. Osborn, M., and K. Weber. 1983. Biology of disease, tumor diagnosis by intermediate filament typing: a novel tool for surgical pathology. *Lab. Invest.* 48:372–394.
23. de Petris, S. 1978. Immunoelectron microscopy and immunofluorescence in membrane biology. *Methods Membr. Biol.* 9:1–201.
24. Pruss, R. M., R. Mirsky, M. C. Raff, R. Thorpe, A. J. Dowding, and B. H. Anderton. 1981. All classes of intermediate filaments share a common antigenic determinant defined by a monoclonal antibody. *Cell.* 27:419–428.
25. Roitt, I. 1977. Essential Immunology. Blackwell Scientific Publications, London. 324.
26. Schiff, P. B, J. Fant, and S. B. Horowitz. 1979. Promotion of microtubule assembly *in vitro* by taxol. *Nature (Lond.).* 277:665–667.
27. Schliwa, M. 1982. Actin of cytochalasin D on cytoskeletal networks. *J. Cell Biol.* 92:79–91.
28. Schliwa, M., and J. van Blerkom. 1981. Structural interaction of cytoskeletal components. *J. Cell Biol.* 90:222–235.
29. Schliwa, M., J. V. Blerkom, and K. R. Porter. 1981. Stabilization of the cytoplasmic ground substance in detergent opened cells and a structural and biochemical analysis of its composition. *Proc. Natl. Acad. Sci. USA.* 78:4329–4333.
30. Sharp, G., M. Osborn, and K. Weber. 1982. Occurrence of two different intermediate filament proteins in the same filament *in situ* within a human glioma cell line. An immunoelectron microscopical study. *Exp. Cell Res.* 141:385–395.
31. Sharp, G., G. Shaw, and K. Weber. 1982. Immunoelectron microscopical localization of the three neurofilament triplet proteins along neurofilaments of cultured dorsal root ganglion neurons. *Cell Res.* 137:403–413.
32. Small, J. V. 1981. Organisation of actin in the leading edge of cultured cells: influence of osmium tetroxide and dehydration on the ultrastructure of actin membrane. *J. Cell Biol.* 91:695–705.
33. Tilney, L. G., D. de Rosier, and M. J. Mulroy. 1980. The organization of actin filaments in the sterocilia of cochlea hair cells. *J. Cell Biol.* 86:244–259.
34. Wang, E., J. G. Cairncross, W. K. A. Yung, E. A. Garber, and R. K. H. Liem. 1983. An intermediate filament-associated protein, p50, recognised by monoclonal antibodies. *J. Cell Biol.* 97:1507–1514.
35. Webster, R. E., D. Henderson, M. Osborn, and K. Weber. 1978. Three-dimensional electron microscopical visualization of the cytoskeleton of animal cells: immunoferritin identification of actin and tubulin containing structures. *Proc. Natl. Acad. Sci. USA.* 75:5511–5575.
36. Wiche, G., H. Herrmann, F. Leichtfried, and R. Pytelia. 1981. Plectin: a high molecular weight cytoskeletal polypeptide component that copurifies with intermediate filaments of the vimentin type. *Cold Spring Harbor Symp. Quant. Biol.* 56:455–463.
37. Willard, M., and C. Simon. 1981. Antibody decoration of neurofilaments. *J. Cell Biol.* 89:198–205.
38. Zumbé, A., C. Stähli, and H. Trachsel. 1982. Association of a M_r 50,000 cap-binding protein with the cytoskeleton in baby hamster kidney cells. *Proc. Natl. Acad. Sci. USA.* 79:2927–2931.